



## PAPER

# Assessing abdominal fatness with local bioimpedance analysis: basics and experimental findings

H Scharfetter<sup>1\*</sup>, T Schlager<sup>2</sup>, R Stollberger<sup>3</sup>, R Felsberger<sup>1</sup>, H Hutten<sup>1</sup> and H Hinghofer-Szalkay<sup>2,4</sup>

<sup>1</sup>Institute for Biomedical Engineering, Technical University Graz, Austria; <sup>2</sup>Institute for Adaptive and Spaceflight Physiology, Austrian Society for Aerospace Medicine, Graz, Austria; <sup>3</sup>Magnetic Resonance Institute, School of Medicine, Karl-Franzens University, Graz, Austria; and <sup>4</sup>Volume Regulation and Space Medicine Research Group, Department of Physiology, School of Medicine, Karl-Franzens University, Graz, Austria

**OBJECTIVE:** Abdominal fat is of major importance in terms of body fat distribution but is poorly reflected in conventional body impedance measurements. We developed a new technique for assessing the abdominal subcutaneous fat layer thickness (SFL) with single-frequency determination of the electrical impedance across the waist (SAI).

**SUBJECTS AND MEASUREMENTS:** The method uses a tetrapolar arrangement of surface electrodes which are placed symmetrically to the umbilicus in a plane perpendicular to the body axis. Twenty-four test subjects (12 male, 12 female) underwent SAI and abdominal magnetic resonance imaging (MRI). The SFL below the sensing electrodes was determined from MRI and correlated with the SAI data at four different frequencies (5, 20, 50 and 204 kHz).

**RESULTS:** A highly significant linear correlation ( $r^2=0.99$ ) between SFL and SAI over a wide range of the abdominal SFL was found. Separate regression models for female and male subjects did not differ significantly, except at 50 kHz.

**CONCLUSION:** SAI represents a good predictor of the SFL and provides an excellent tool for the assessment of central obesity. *International Journal of Obesity* (2001) 25, 502–511

**Keywords:** abdominal bioimpedance; central obesity; fat layer thickness

### Introduction

Cardiovascular diseases remain a leading cause of morbidity and mortality. Besides other risk factors like hypertension, dyslipidemia and history of smoking, an android distribution of adipose tissue has been identified as correlated to incidence of cardiovascular complications.<sup>1–4</sup> Many longitudinal studies, the Framingham study probably being the best known of all,<sup>5</sup> have assessed individual cardiovascular risk in relation to nutritional and metabolic factors.

A positive association between the pattern of body shape and the occurrence of cardiovascular complications such as stroke, angina pectoris, myocardial infarction and death from coronary heart disease has been shown by prospective studies.<sup>6–8</sup> Adequate anthropometric screening can help to identify those at elevated risk, and potentially prevent

unfavorable development and premature death. Waist-to-hip ratio determination has been proven useful to assess central obesity and predict cardiovascular risk and metabolic alterations.<sup>9,10</sup>

A more direct, sensitive method to assess central obesity could be particularly useful in clinical and occupational medicine to find subjects with a cluster of multiple risk factors including hypercholesterolemia, hypertension, diabetes and glucose intolerance.

Established body fat assessments all suffer from drawbacks: underwater-weighting<sup>11,12</sup> is a relatively inconvenient procedure which estimates total fat content, not regional fat distribution, and is based on the assumption of certain fat/lean mass densities, according to normal references. These references may not be valid in hydration disorders or other pathology.  $K^{40}$  scintillation counting<sup>12,13</sup> is accurate but highly difficult to perform; again, fat distribution escapes assessment. Imaging methods like CT and MRI<sup>14–17</sup> yield accurate regional fat data but are extremely costly and unsuited for self-monitoring in a private setting. Ultrasound subcutaneous fat layer measurements require considerable skills.<sup>18</sup> The TOBEC method<sup>19</sup> uses quite expensive

\*Correspondence: H Scharfetter, Institute for Biomedical Engineering, Technical University Graz, Inffeldgasse 18, A-8010 Austria.  
E-mail: scharfetter@bmt.tu-graz.ac.at  
Received 20 April 2000; revised 18 September 2000;  
accepted 11 October 2000

instrumentation and is based on an empirical approach which is poorly based on theoretical grounds.

The measurement of the electrical impedance of defined body segments could be an inexpensive and easily applicable alternative. Two different approaches have been suggested:

- Single-frequency bioimpedance analysis (BIA)<sup>13,20</sup> of the whole body or of different body segments at one frequency, most commonly at 50 kHz. The body fat content is calculated from the measured impedance with an empirical formula which, in most cases, has been obtained by linear regression analysis.
- Bioimpedance spectroscopy (BIS):<sup>21</sup> the principle is the same as that of BIA, however the impedance is measured at multiple frequencies between some kHz and up to 1 MHz. This method is primarily used for the determination of body fluid volumes and fat-free mass.

The basic disadvantage of conventional impedance approaches is that an inherently error-prone quantity—fat free mass to be subtracted from total body weight—must be used for adipose tissue assessment. Another drawback of established impedance-based method is a low sensitivity to regional, for example subcutaneous abdominal, fat. Whole body impedance contains little information about the trunk,

which contributes only 5–10% to total impedance<sup>22</sup> and this problem also holds for impedance measurement between both feet of the subject. In both cases the electrical current passes mainly through fat-free, highly conducting tissue; only in considerably obese people does fat significantly contribute to overall conductance as recently analyzed by Baumgartner *et al.*<sup>23</sup>

The indirect approach renders the methods susceptible for interferences with all physiological quantities which determined the electrical properties of the well-conducting tissues, for example muscle.

Alternatively the subcutaneous fat layer thickness (SFL) may be estimated by transimpedance measurement between two pairs of electrodes attached directly above the region of interest.<sup>24</sup> This technique has also been suggested recently for an electronic skinfold caliper (for a review see Elia and Ward<sup>25</sup>). An alternating current with constant amplitude is injected into the outermost electrode pair and the resulting voltage drop between the innermost electrodes is measured in order to calculate the impedance. The configuration used in our study is depicted in Figure 1.

As the current passes transversally through the abdomen, the potential difference measured on the surface is determined by the geometry of the region's different tissue layers. Fat is significantly less conducting than, for example, muscle

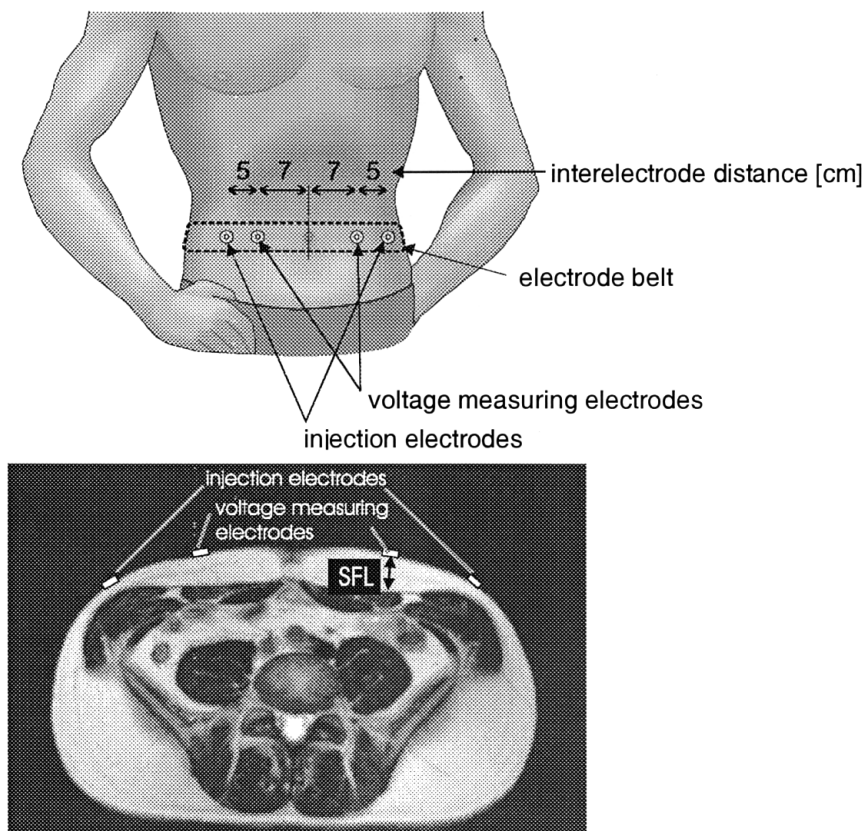


**Figure 1** Electrode location and spacing, frontal view (upper panel) and transversal MRI-cross-section with the definition of SFL (lower panel).

or other tissues,<sup>26</sup> hence the major part of the potential drop occurs in the close vicinity of the injection electrodes. Sensing electrodes which are attached very near the injection electrode pick up voltages which are mainly determined by the fat layer. The spacing shown in Figure 1 also yields a considerable sensitivity to deeper structures, in particular to the abdominal muscles and the mesentery. Hence the visceral fat content is also partly reflected in the measured transimpedance. In contrast to whole-body measurements, the resulting impedance signal is very sensitive to the local fat content and less susceptible for interferences, in particular fluid shifts in the extremities.

## Procedure and methods

### Subjects

Twelve men (22–53 y, 50–137 kg, 175–185 cm, BMI 16–42 kg/m<sup>2</sup>) and 12 women (19–52 y, 45–114 kg, 159–180 cm, BMI 16.5–40.4 kg/m<sup>2</sup>) participated, fully informed about the purpose and nature of the experiments, after giving their informed consent. The anthropometrical data are listed in Table 1.

### Experimental protocol

The investigations, comprising NMR-imaging and a series of impedance measurements, were performed on different days between 17 00 and 19 30 h. The total measurement time for one subject was about 50 min. Impedance measurements were carried out no more than 30 min before NMR imaging. Data recording started after a period of 15 min in supine rest in order to minimize the influence of orthostatic fluid shifts.<sup>27</sup> During the abdominal measurement the subjects were asked to hold their breath in order to avoid movement artifacts. To assess the magnitude of orthostatic effects, measurements were repeated in the upright position in the male subjects. Room temperature was kept constant at 24 ± 1°C throughout the experiments.

### Impedance measurements

A Xitron 4000B was used for impedance measurements (Xitron Technologies Inc., San Diego, USA). Four commercial ECG-electrodes (Ag/AgCl, Swaromed REF1023, Nessler Medizintechnik, Austria) were attached in a symmetric fashion left and right of the umbilical midline at the height of the iliac crest, exactly positioned with a belt according to Figure 1. A constant current of 250 µA was injected. The electrode placing was different from that applied in Gonzalez *et al.*<sup>24</sup> In particular the spacing is wider in order to increase the sensitivity for deeper structures, for example the mesentery. It must be admitted, however, that the choice of the spacing was somewhat *ad-hoc* and that it may be optimized in future investigations.

To arrive at reliable impedance data between 10 and 100 Ω, the voltage measurement range of the XITRON 4000B was extended with a special preamplifier (gain = 10). Samples were taken at 50 logarithmically spaced frequencies from 5 to 500 kHz. Each data acquisition procedure lasted for about 20 s. The whole arrangement was thoroughly calibrated before each measurement with an RC-network in order to keep the error of the measuring electronics < 1% in the whole frequency range. This calibration does, however, not correct for stray capacitances between the subject and ground so that during the *in-vivo* measurement the error can be bigger. Moreover the presence of a thick fat layer below the electrodes in combination with the input impedance of the analyzer introduces similar effects to a high electrode impedance so that the data can become highly unreliable at frequencies above 200 kHz. For this reason data above 204 kHz were excluded from statistical analysis.

### Reference measurements by MRI

SFL was assessed from transversal MRI-cross sections obtained at the height of the electrode belt, as the mean of the shortest distances between the fat layer's outer and inner boundary below the voltage measuring electrodes. MRI was performed on a 1.5 T system (Philips ACS-NT, The Nether-

**Table 1** Test subject's anthropometrical data

Male				Female			
No.	Height (cm)	Mass (kg)	BMI (kg/m <sup>2</sup> )	No.	Height (cm)	Mass (kg)	BMI (kg/m <sup>2</sup> )
1	188.0	124.0	35.1	1	168.0	114.0	40.4
2	175.0	50.1	16.4	2	159.0	48.0	19.0
3	180.5	87.2	26.8	3	178.0	78.9	24.9
4	184.0	80.5	23.8	4	175.5	71.2	23.1
5	180.0	102.5	31.6	5	167.0	62.1	22.3
6	178.5	77.3	24.3	6	166.0	63.9	23.2
7	185.0	84.7	24.7	7	180.0	75.1	23.2
8	187.0	78.2	22.4	8	170.0	77.1	26.7
9	180.5	76.9	23.6	9	165.0	51.2	18.8
10	180.0	137.1	42.3	10	164.5	44.6	16.5
11	180.0	80.0	24.7	11	168.0	66.8	23.7
12	170.0	64.2	22.2	12	169.0	54.1	18.9

lands) with the circularly polarized body resonator. Scan planning was performed on sagittal and coronal scout scans. For the study, a  $T_2$ -weighted multi-slice Turbo-Spin-Echo sequence was used ( $TR/TE=3000/115$ , field-of-view=350–450 mm, slice thickness=10 mm, number of slices=23, serial averaging, signal averages=4, respiratory triggering).

### Statistics and data interpretation

Data preprocessing and BIA estimation were performed with MATLAB™ (Mathworks Inc., Natick). As the performance of the method turned out to be essentially equal at all frequencies below 250 kHz (see section 'results') the analysis was carried out for only four frequencies in order to reduce the effort for statistical evaluation. Those frequencies (5, 20, 50 and 204 kHz) were selected according to the following criteria: limitation of the highest frequency to about 200 kHz (reliability of data), inclusion of the widely used 50 kHz and preferred evaluation at low frequencies (5 and 20 kHz) in order to reduce the influence of stray capacitances. The abdominal transimpedance modulus was tested for linear correlation with the SFL determined with MRI. In the following the transimpedances are referred to as  $Z_5$ ,  $Z_{20}$ ,  $Z_{50}$  and  $Z_{204}$ . Separate regression models were calculated for males (model  $m$ ), females (model  $f$ ), and the total population (model  $t$ ). It was tested whether  $m$  and  $f$  differed significantly from each other by assuming the following null hypothesis. If both groups can be described by the same model ( $m$ ) then the residuals between model prediction and measured data should be zero and should not differ significantly from each other. After checking the normality of the residuals by inspection of the lognormal plot the Levene test for equality of variances and the two-tailed  $t$ -test for equality of the means were carried out. The statistical analysis was done with SPSS™ 9.0 for Windows™ (SPSS Inc., Chicago, USA).

The residuals for standing and supine position (male subjects) were tested for equality of the variances at 50 kHz (Levene test).  $P < 5\%$  was considered as statistically significant for rejecting the null hypothesis in all tests.

### Reproducibility

Bioimpedance data are subject to a certain variability due to a number of reasons, for example postural changes, changes of the skin temperature, variance of the electrode impedance and errors in the electrode placement. In particular, the latter causes a certain intra- and inter-operator variability in the case of repetitive measurements. In addition to the postural changes we checked for the error caused by electrode impedance and electrode displacement.

**Electrode impedance.** The impedance between the voltage sensing electrodes was measured in bi- ( $Z_{bi}$ ) and tetrapolar configuration ( $Z_{tetra}$ ) according to Newell *et al.*<sup>28</sup>  $Z_{el}$  can then be estimated by:

$$Z_{el} = \frac{Z_{bi} - Z_{tetra}}{2} \quad (1)$$

The error caused by  $Z_{el}$  was then estimated from a lookup-table which had been generated experimentally with a special RC-phantom similar to that used in Scharfetter *et al.*<sup>29</sup> This phantom mimicks the abdominal transimpedance together with variable electrode impedances and all important stray capacitances.

### Electrode placement between different measurements.

Experiments were carried out in only two persons (one male, one female, 23 and 25 y, 68 and 83 kg, 172 and 192 cm, respectively) because similar data were published previously for whole-body and segmental arrangements.<sup>30</sup> So it was just checked whether the data range was comparable. In addition to the configuration in Figure 1 electrodes were placed 2 cm right from the original positions in order to simulate a transversal displacement. For the simulation of longitudinal displacement and rotation, another four electrodes were attached 2 cm caudal from the original positions. Impedances were measured for the original positions, translation towards right and caudal as well as for clockwise rotation. For the rotation the right caudal electrode pair was connected to the analyzer instead of the original pair. The error due to an electrode displacement was defined as the difference between the impedances with original and displaced electrodes, respectively.

### Results

As shown in Figure 2 the modulus of the impedance spectra changes significantly with the SFL. The morphology of the spectra matches essentially that which is known from muscle tissue.<sup>31</sup>

The SFL measured with MRI and the impedance exhibit a highly significant linear correlation at all frequencies. Figure 3 shows the results for model  $t$  at 50 kHz. The correlation coefficient increases slightly with the frequency ( $r^2=0.97$  at 5 kHz to  $r^2=0.984$  at 204 kHz). The slope of the regression line increases monotonically with the frequency from 1.07 to 1.13, whereas the intercept decreases from 21.3 to 7.8. The confidence intervals of the prediction decreases slightly with increasing frequency.

The results of the  $t$ -test for comparing models  $m$  and  $f$  are summarized in Table 2. Only at 50 kHz did the models  $m$  and  $f$  not differ significantly from each other, which is also reflected in the Bland–Altman plot for model  $m$  at 50 kHz in Figure 4.

In Figure 4 the outlier no. 12 appears close to the line, 'mean – 2s.d.'. The residuals for the remaining male subjects remain lower than 10% of the SFL at SFL-values > 20 mm. As the absolute residuals did not decrease with decreasing SFL the percent deviations become large at low SFL-values, ie in very lean subjects. The female subjects showed a slightly larger scatter than the male ones.

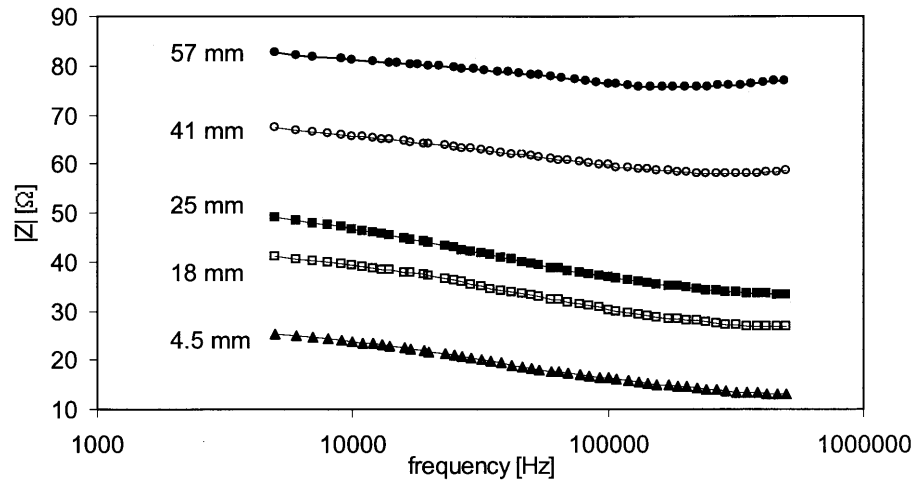


**Figure 2** Dependence of the impedance spectra on the SFL. Five selected male cases shown.

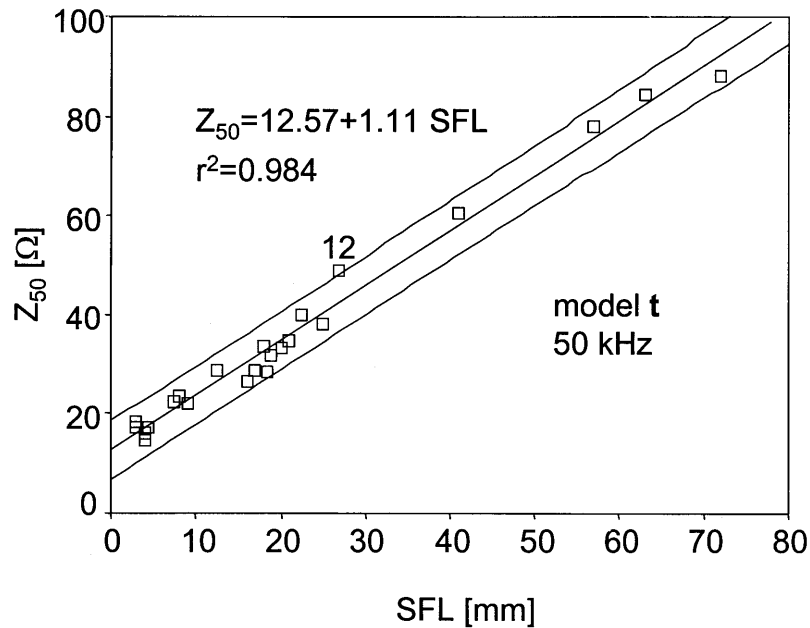


**Figure 3** SFL-impedance correlation from pooled data (model t) at 50 kHz. The figure depicts the regression line and the 95% prediction intervals. One outlier is labelled with its subject number (12).

Finally the prediction formula for the SFL from  $Z_{50}$  was obtained by regression of SFL vs  $Z_{50}$  and was found as:

$$\text{SFL (mm)} = 0.89 Z_{50} (\Omega) - 10.84 \quad (2)$$

### Reproducibility

**Electrode impedance.** The measured contact impedances of the ECG electrodes varied between 400 and 2000  $\Omega$ . The respective error of the impedance modulus remained always

below 1% in the specified frequency range of the XITRON 4000B except at very low (< 10 kHz) and high (> 300 kHz) frequencies. The optimum frequency lay around 100 kHz.

**Postural changes.** Data from the male subjects correlated worse in the upright than in the supine position ( $r^2 = 0.98$  vs 0.996), as shown for 50 kHz in Figure 5. The variance of the residuals was significantly higher for the standing subjects (s.d.) = 3.6  $\Omega$  vs 1.4  $\Omega$ ). Also the slope of the regression line is slightly altered by the postural change.

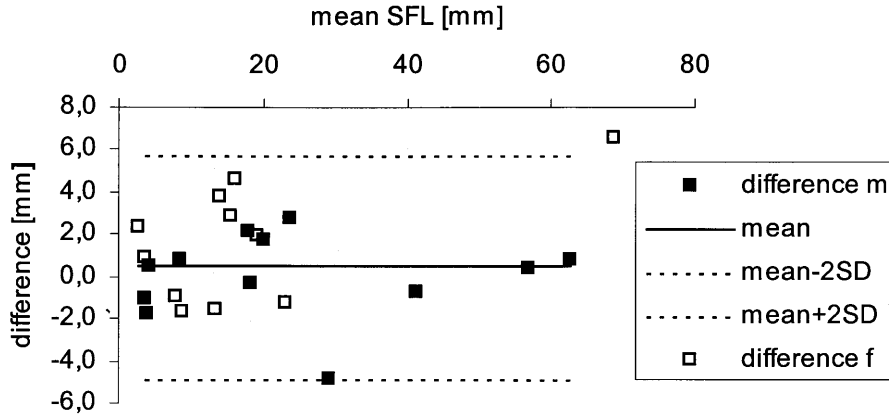


Figure 4 Bland–Altman plot for model *m* at 50 kHz.

**Table 2** Regression model *f* and *m* parameters. Asterisk ‘\*’ in ‘Difference’ column indicates that models are significantly different ( $P < 0.05$ )

Frequency (kHz)	Slope ( $\Omega/\text{mm}$ )		Intercept (mm)		$r^2$		Difference
	<i>f</i>	<i>m</i>	<i>f</i>	<i>m</i>	<i>f</i>	<i>m</i>	
5	1.00	1.08	20.1	23.3	0.98	0.98	*
20	1.13	1.09	16.3	18.7	0.99	0.90	*
50	1.05	1.14	12.6	12.8	0.99	0.99	
204	1.17	1.17	7.5	8.5	0.9	0.99	*

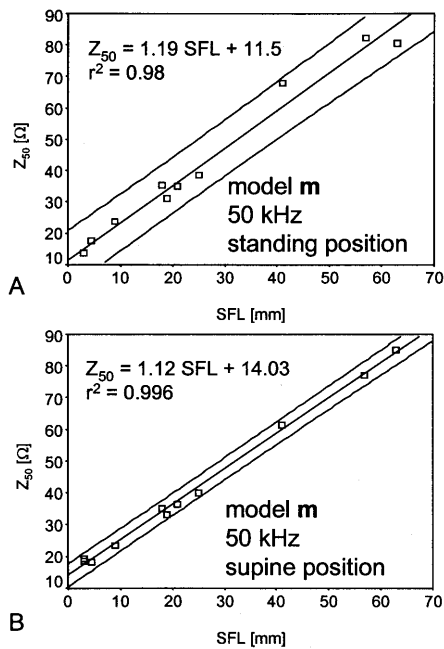


Figure 5 Correlation between SFL and impedance at 50 kHz in standing (A) and supine (B) position. The regression lines are shown with the 95% prediction confidence bands.

Inspection of the residuals in Figure 6 reveals that the increased variance in the standing position is nearly entirely due to subjects with high SFL. The relative deviation became higher than 10% in subjects with SFL < 18 mm and SFL > 40 mm.

**Electrode dislocations.** Electrode dislocations by 1 cm yielded errors of up to 5% in the case of a translation perpendicular to the body axis. Longitudinal translation as well as a rotation of the electrode belt (corresponding to a  $\pm 0.5$  cm longitudinal displacement of both outermost electrodes) produced errors of less than 2.5%.

### Discussion

Recent evidence suggests that cardiovascular health is strongly linked to metabolic health and body shape, with ‘apples’ and ‘pears’ differing in risk potential.<sup>6–10,32–35</sup> Easily determined predictive anthropometric criteria are waist circumference<sup>36</sup> and waist-to-hip ratio. A more sophisticated while easily applicable method, capable of differentiating fat and non-fat abdominal tissue, can be expected to provide added benefit in identifying those with a cluster of multiple risk factors including hypercholesterolemia, hypertension, diabetes and glucose intolerance.

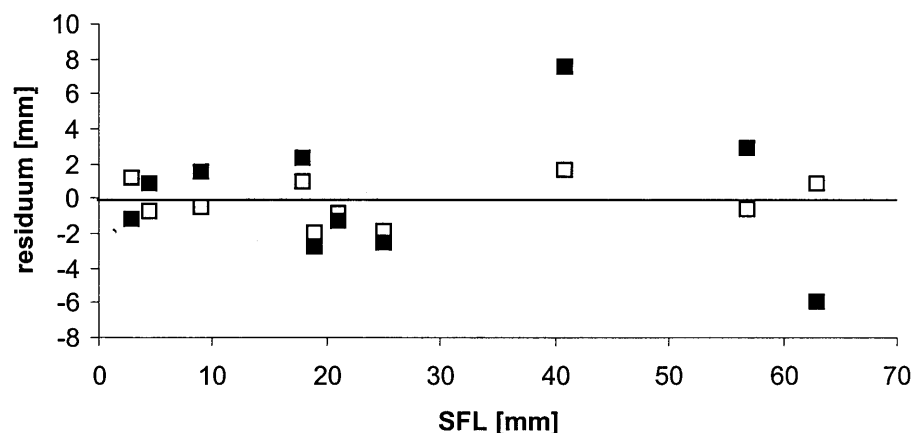


**Figure 6** Residuals for the linear regression of the male subjects when standing (filled squares) and supine (open squares).

'Bioimpedance' measurement strategies currently in use rely on an inherently error-prone approach: the assessment of fat-free mass, through which the current mainly passes. Adipose tissue is then estimated from whole body lean mass. Worse, the trunk impedance contributes only 5–10% to total impedance as measured with hand-to-foot or foot-to-foot electrode placement. A separation into subcutaneous and visceral fat is virtually impossible. We present a measurement strategy which obviously gives a good estimate of abdominal subcutaneous fat. This approach, in combination with other modalities for the estimation of central obesity (for example segmental BIA, determination of the waist circumference etc) may give a better index for the abdominal fat distribution than established screening methods. However, the number of subjects is still small and thus we consider the presented work as a promising pilot-study. In future investigations we will focus on cross-validation of our prediction formula in a second subject cohort.

#### Limitations of the method

At very high values of the SFL the shape of the impedance spectra deviates slightly from the typical spectrum for muscle.<sup>31</sup> In particular the impedance modulus increases again at high frequencies in very obese subjects as shown in Figure 2. This behavior is not expected from biological tissues and in fact represents an artifact. It is known that high electrode impedances cause spurious dispersions in the high-frequency range. These dispersions are due to capacitive leakage currents via stray capacitances in the measuring electronics.<sup>29</sup> A similar effect can occur during measurements on a layered extended object if the outer layer (here the subcutaneous fat) consists of poorly conducting material such as adipose tissue. Such a layer mimicks a high impedance between the muscular compartment and the electrode leads and can thus provoke similar effects as a high electrode impedance. Therefore high-frequency data should not be used for further analysis in subjects with high SFL. The

observed increase of the slope of the regression line with frequency is probably at least partially caused by this artifact. According to the presented data the narrowest prediction intervals are obtained at 50 kHz, which makes this frequency well suited for single frequency analysis.

The largest relative errors were observed at SFL values < 20 mm (lean subjects). Thus the method reaches its highest accuracy at SFLs > 30 mm, with a relative error < 10%. At an NMR image pixel size of about 1 mm<sup>2</sup> the discretization error can become high for very thin subjects, an effect which may have partly contributed to the observed deviations at SFLs < 5 mm. Moreover we defined SFL simply as the distance between inner and outer fat layer boundary below the voltage measuring electrode; considering this, the good correlation and the comparatively low scatter of the data is surprising.

The regression was less stringent when the subjects were upright, primarily corresponding to data from SFL > 40 mm (Figure 6). We assume the reason to be the geometry of the measured region with postural change, which varies much more in obese than in lean people. More accurate data seem to result from supine measurements.

#### Reproducibility

**Electrode impedance.** The measured electrode impedances are in good agreement with data published in Zipp<sup>37</sup> for 5 kHz (1–5 kΩ). The related error of less than 1% up to 300 kHz is small compared to other sources of artifacts and can thus be neglected.

**Postural changes.** Regarding the differences between the data obtained for standing and supine male subjects (Figure 6) the relative difference becomes bigger than 10%, especially for the obese and for the very lean persons. This discrepancy demonstrates the necessity for measurements in a standardized (for example the supine) position after a certain equilibration time (15 min).

**Electrode displacement.** In our two subjects we observed similar impedance changes as reported in Lozano *et al.*<sup>30</sup> where electrode dislocations by up to 1 cm caused a  $\Delta Z_{rel,disp}$  of up to 4.4% on arms and legs. The main reason for the displacement error is probably the change of the geometrical boundary conditions for the current field. The distance between inner and outer boundary of the fat layer below the current injection electrodes varies considerably in the case of a transversal electrode shift. This, however, means a significant change of the current path and hence of the transimpedance. A longitudinal shift has obviously less impact on the impedance as the geometry varies less along the body axis.

The overall reproducibility depends on all the discussed effects. Errors due to postural changes can be reduced significantly by applying a standardized measurement protocol such that the most important source of variability is the electrode positioning error. Regarding our results and the data known from literature a 1 cm displacement leads to errors in the range of 5%, which would be acceptable for many applications. However, due to the small subject number our reproducibility check cannot be considered as exhaustive and a more elaborate study with repeated mea-

surements including inter- and intra-operator tests remains to be carried out in order to confirm the estimated error limits.

#### Data interpretation

We did not expect a linear relationship between abdominal transimpedance and SFL since the theory of vertical electric sounding would predict otherwise: On a porcine skin plus adipose tissue phantom, mounted on a conducting substrate, a symmetric electrode configuration (4 mm voltage sensing electrode spacing, 10–56 mm distance between current injection electrodes) resulted in a pronounced non-linear relationship between transimpedance and fat layer thickness.<sup>24</sup> However, our electrode spacing was completely different. Obviously in our setup a linear relationship can be applied over a wide range of validity. In our setup not only the SFL but also the muscles and the mesenteric compartments contribute to the measured transimpedance. It is thus postulated that the general non-linear correlation is linearized due to these contributions from deeper adipose structures, for example the mesentery. This feature renders the

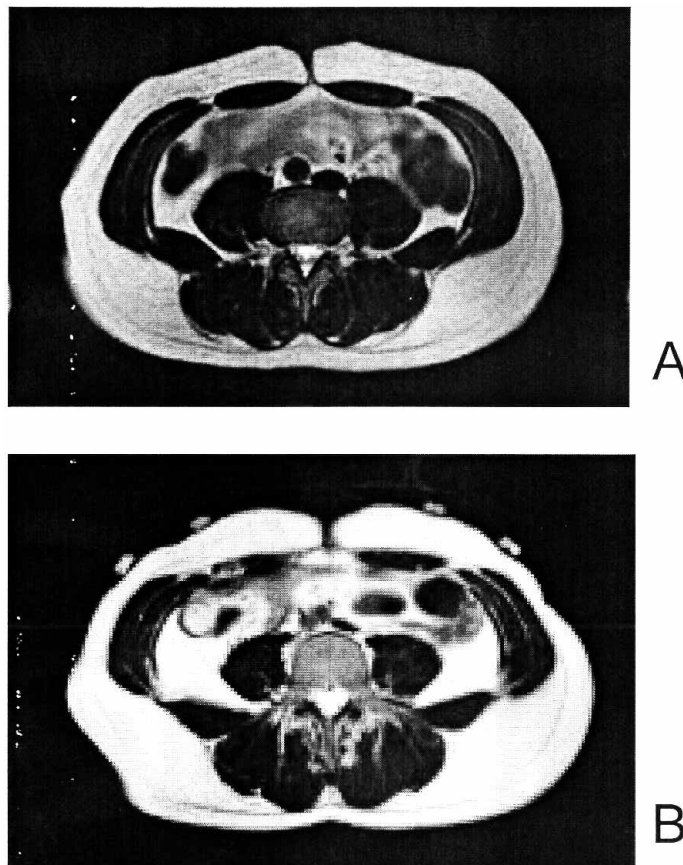


**Figure 7** (A) NMR image of subject 7. (B) NMR image of subject 12.

proposed arrangement particularly attractive for a simple data analysis.

Although the correlation between SFL and  $Z_{50}$  is in general excellent, one outlier (subject 12: Table 1) has been observed. Figure 7 shows the NMR-cross-sections of the two male subjects 7 and 12, who had a comparable SFL. Obviously the distance between inner and outer fat boundary is virtually equal below the voltage sensing electrode. However, the distance below the current injection electrode is much smaller in subject 12, which means a much lower voltage drop along the current path between electrode and muscle tissue. Moreover the muscle mass is much lower and the visceral fat content appears to be higher in subject 12. This suggests different field geometry and hence different transimpedance. We suppose that the impedance is influenced by the following structural factors:

- the visceral fat content;
- the geometry of the fat layer below the electrodes;
- the abdominal muscle mass.

In conclusion our study demonstrates excellent prediction of subcutaneous abdominal fat layer thickness (SFL) by an easy applicable single-frequency electrical abdominal impedance (SAI) measurement across the waist. Magnetic resonance imaging of the abdomen was used as a reference; the results demonstrate a highly significant linear correlation between SFL and SAI over a wide range of abdominal SFL—from extremely lean to considerably obese. The big advantage of local impedance determination over whole-body measurements is that the measured signal is very sensitive to the local fat content and hence is less susceptible to non-specific influences such as body fluid shifts in peripheral compartments. The method provides comparatively low relative errors, especially in the obese. The shown approach is the simplest possible way to obtain information about the SFL and this simplicity makes it attractive for the practical use. The application of more complex data acquisition strategies with multifrequency measurements and three voltage sensing electrodes may even render possible to discern the contributions from different compartments (subcutaneous fat, visceral fat, muscle). In particular the SFL may become clearly distinguishable from deeper compartments by combining our electrode arrangement with the electronic skinfold calliper.<sup>25</sup> The potential of such an approach will be tested in future investigations by applying more elaborate electrical models.

#### Acknowledgements

Experiments were done at Institute for Adaptive and Spaceflight Physiology, Austrian Society for Aerospace Medicine (ASM), Graz, Austria. The authors thank Ulrike Marauli, Andreas Rothaler and Melitta Unterlerchner for their excellent technical support.

#### References

- 1 Björntorp P. Metabolic implications of body fat distribution. *Diabetes Care* 1991; **14**: 1132.
- 2 Després JP, Moorjani S, Lupien PJ, Tremblay A, Nadeau A, Bouchard C. Regional distribution of body fat, plasma lipoproteins and cardiovascular disease. *Arteriosclerosis* 1990; **10**: 497–511.
- 3 Krotkiewski M, Björntorp P, Sjöström L, Smith U. Impact of obesity on metabolism in men and women. Importance of regional adipose tissue distribution. *J Clin Invest* 1983; **72**: 1150–1162.
- 4 Vague P. The degree of masculine differentiation of obesities: a factor determining predisposition to diabetes, atherosclerosis, gout and uric calculous disease. *Am J Clin Nutr* 1956; **4**: 20–34.
- 5 Anderson KM, Wilson PWF, Odell PM, Kannel WB. An updated coronary risk profile. A statement for health professionals. *Circulation* 1991; **83**: 356–362.
- 6 Donahue RP, Abbott RD, Bloom E, Reed DM, Yano K. Central obesity and coronary heart disease in men. *Lancet* 1987; **21** (8569): 821–824.
- 7 Ducimetiere P, Richard J, Cambien F. The pattern of subcutaneous fat distribution in middle-aged men and the risk of coronary heart disease: the Paris prospective study. *Int J Obes* 1986; **10**: 229–240.
- 8 Twisk JWR, Kemper HCG, van Mechelen W, Post GB, van Lenthe FJ. Body fatness: longitudinal relationship of body mass index and the sum of skinfolds with other risk factors for coronary heart disease. *Int J Obes Relat Metab Disord* 1998; **22**: 915–922.
- 9 Larsson B, Svärdsudd K, Welin L, Wilhelmsen L, Björntorp P, Tibblin G. Abdominal adipose tissue distribution, obesity and risk of cardiovascular disease and death: 13 year follow up of participants in the study of men born 1913. *Br Med J* 1994; **288**: 1401–1404.
- 10 Megnien JL, Denarie N, Cocaul M, Simon A, Levenson J. Predictive value of waist-to-hip ratio on cardiovascular risk events. *Int J Obes Relat Metab Disord* 1999; **23**: 90–97.
- 11 Akers R, Buskirk ER. An underwater weighing system utilizing 'force cube' transducers. *J Appl Physiol* 1969; **26**: 649–652.
- 12 Forbes GB. *Human body composition*. Springer: New York; 1987.
- 13 Lukaski HC. Methods for the assessment of human body composition: traditional and new. *Am J Clin Nutr* 1987; **46**: 537–556.
- 14 Fuller MF, Fowler PA, McNeill G, Foster MA. Imaging techniques for the assessment of body composition. *J Nutr* 1994; **124**: S1546–1550.
- 15 Sjöström L, Kvist H, Cederblad A, Tylen U. Determination of total adipose tissue and body fat in women by computed tomography, <sup>40</sup>K, and tritium. *Am J Physiol* 1986; **250**: E736–745.
- 16 Sohlstrom A, Wahlund LO, Forsum E. Adipose tissue distribution as assessed by magnetic resonance imaging and total body fat by magnetic resonance imaging, underwater weighing, and body-water dilution in healthy women. *Am J Clin Nutr* 1993; **58**: 830–838.
- 17 Thomas EL, Saeed N, Hajnal JV, Brynes A, Goldstone AP, Frost G, Bell JD. Magnetic resonance imaging of total body fat. *Appl Physiol* 1998; **85**: 1778–1785.
- 18 Abe T et al. Total and segmental subcutaneous adipose tissue volume measured by ultrasound. *Med Sci Sports Exercise* 1996; **28**: 908–912.
- 19 Harrison GG, Van Atallie TB. Estimation of body composition: a new approach based on electromagnetic principles. *Am J Clin Nutr* 1982; **35**: 1176–1179.
- 20 Kushner RF. Bioelectrical impedance analysis: a review of principles and applications. *J Am Coll Nutr* 1992; **11**: 199–209.
- 21 Van Loan MD, Withers P, Matthie J, Mayclin PL. Use of bio-impedance spectroscopy (BIS) to determine extracellular fluid (ECF), intracellular fluid (ICF), total body water (TBW), and fat-free mass (FFM). In: Ellis, KJ, Eastman JD (eds). *Human body composition: in vivo methods, models, and assessment*. Plenum: New York; 1993.
- 22 Organ LW, Bradham GB, Gore DW, Lozier SL. Segmental bioelectrical impedance analysis: theory and application of a new technique. *J Appl Physiol* 1994; **77**: 98–112.

- 23 Baumgartner RN, Ross R, Heymsfield SB. Does adipose tissue influence bioelectric impedance in obese men and women? *J Appl Physiol* 1998; **84**: 257–262.
- 24 Gonzalez CA, Zuniga O, Padilla LE. Detection of animal tissue thickness using simple vertical electric sounding (VES). *Physiol Measmt* 1997; **18**: 85–91.
- 25 Elia M, Ward LC. New techniques in nutritional assessment: body composition methods. *Proc Nutr Soc* 1999; **58**: 33–38.
- 26 Geddes LA, Baker LE. The specific resistance of biological material—a compendium of data for the biomedical engineer and physiologist. *Med Biol Engng* 1967; **5**: 271–293.
- 27 Scharfetter H, Monif M, Laszlo Z, Lambauer T, Hutten H, Hinghofer-Szalkay H. Effect of postural changes on the reliability of volume estimations from bioimpedance spectroscopy data. *Kidney Int* 1997; **51**: 1078–1087.
- 28 Newell JC, Isaacson D, Gisser DC. Rapid assessment of electrode characteristics for impedance imaging. *Biomed Engng* 1990; **37**: 735–738.
- 29 Scharfetter H, Hartinger P, Hinghofer-Szalkay H, Hutten H. A model of artifacts produced by stray capacitance during whole body or segmental bioimpedance spectroscopy. *Physiol Measmt* 1998; **19**: 247–261.
- 30 Lozano A, Rosell J, Pallas-Areny R. Errors in prolonged electrical impedance measurements due to electrode repositioning and postural changes. *Physiol Measmt* 1995; **16**: 121–130.
- 31 Rigaud B, Hamzaoui L, Frikha MR, Chauveau N, Morucci JP. In vitro tissue characterization and modelling using electrical impedance measurements in the 100 Hz–10 MHz frequency range. *Physiol Measmt* 1995; **16**(3 Suppl A): A15–28.
- 32 Rexrode KM, Carey VJ, Hennekens CH, Walters EE, Colditz GA, Stampfer MJ, Willett WC, Manson JAE. Abdominal adiposity and coronary heart disease in women. *JAMA* 1998; **280**: 1843–1848.
- 33 Eckel RH, Krauss RM. American Heart Association call to action: obesity as a major risk factor for coronary heart disease. *Circulation* 1998; **97**: 2099–2100.
- 34 Molarius A, Seidell JC, Sans S, Tuomilehto J, Kuulasmaa K. Waist and hip circumferences, and waist-hip ratio in 19 populations of the WHO MONICA project. *Int J Obes Relat Metab Disord* 1999; **23**: 116–125.
- 35 Okosun IS, Prewitt TE, Liao Y, Cooper RS. Association of waist circumference with ApoB to ApoAI ratio in black and white Americans. *Int J Obes Relat Metab Disord* 1999; **23**: 498–504.
- 36 Han TS, van Leer ED, Seidell JC, Lean MEJ. Waist circumference as a screening tool for cardiovascular risk factors: evaluation of receiver operating characteristics (ROC). *Obes Res* 1996; **4**: 533–547.
- 37 Zipp P. Die Bemessung der Elektroden-Haut-Kontaktfläche und der Verstärkereingangsimpedanz bei der quantitativen Oberflächenelektrographie (EKG und EMG). *Biomed Technol* 1978; **23**: 130–140.